PO.142

# Should we really be concerned about obstacles in wind resource assessment

DTU Wind Energy
Department of Wind Energy

**Alfredo Peña, Andreas Bechmann, Davide Conti, Nikolas Angelou, Torben Mikkelsen, Peggy Friis**
DTU Wind Energy, Technical University of Denmark, Roskilde, Denmark

## Introduction

The shelter behind obstacles is one of the most complex flows to measure and to model and so its study is important in applications such as wind energy. However, during the exponential-growth period of the wind industry, the shelter did not significantly represent an issue for turbine energy-yield estimation because the machines were sited in free-shelter regions. Currently, due to the less available 'best' wind sites, many turbines are deployed close to obstacles. Also the small wind industry has grown and in some countries, due to planning rules, small wind turbines are placed very close to houses, representing an increase of the sheltering effects. Here we present a dataset of full-scale measurements of the shelter behind a 3-m tall and 30-m wide solid fence, which were performed at DTU's Risø campus in Roskilde, Denmark. The measurements were conducted by the short-range WindScanner (WS) system (http://www.windscanner.dk), where three synchronized wind lidars measured the 3D wind velocity vector on a vertical-plane grid behind the fence. The measurements represent a wide variety of atmospheric conditions, and different cases are analyzed as function of the relative direction of the fence to the inflow. These cases present a unique opportunity to evaluate shelter models.


Figure 1: The fence experiment (left) on the area surrounding DTU's test station, (middle) with the instrumentation including the lidars and the mast, and (right) scanning configuration

## Methods and inflow conditions

The shelter is studied in terms of the speed up, $U(z)/U_o(z)$, where the subscript $_o$ refers to the inflow value. The inflow characteristics are estimated using the diabatic wind profile,

$$U_o(z) = \frac{u_*}{\kappa}\left[\ln\left(\frac{z}{z_o}\right) - \phi_m(z/L)\right]. \quad (1)$$

The cases represent the average shelter over direction intervals centered at three increasing relative directions $\theta$s:

| Case | $\theta$ [deg.] | $z_o$ [m] | $u_*$ [m s$^{-1}$] | $z/L$ | No. of full scans |
|---|---|---|---|---|---|
| I | $0 \pm 15$ | 0.0016 | 0.36 | 0.021 | 159 |
| III | $-30 \pm 15$ | 0.0037 | 0.34 | 0.023 | 604 |
| IV | $-60 \pm 15$ | 0.0131 | 0.39 | 0.045 | 583 |

The roughness length $z_o$ is estimated from Eq. 1 using one month of 10-min statistics from sonic measurements at 6 and 12 m on the mast besides the fence (Fig. 1-right) and a median $z_o$ is computed within 10° intervals. $z_o$ in the table is the ensemble average of the $z_o$ medians within the corresponding $\theta$ intervals of each case. The friction velocity $u_*$ in the table is estimated from Eq. 1 assuming $\psi_m = 0$ and using the ensemble-average 6-m sonic mean wind, which is computed within the period of each WS full-scan (i.e. a complete measurement at the 217 scanning positions on the grid in Fig. 1-right), and ensemble-averaged for the full-scans belonging to each case. The inflow profile estimated using Eq. 1 with $\psi_m = 0$ shows good agreement with the two sonics (not shown). The table includes the ensemble-average $z/L$ found by averaging the 10-min 6-m sonic fluxes concurrent with the full-scans. Figure 2 shows an intercomparison of $U$ measured by the 6-m sonic and the WS scanning grid point closest to the fence and at $z \approx 6$ m, and the difference between these two measurements as function of $\theta$. The figure illustrates that the sonic and the WS agree well for the directions where the fence is in downwind conditions.

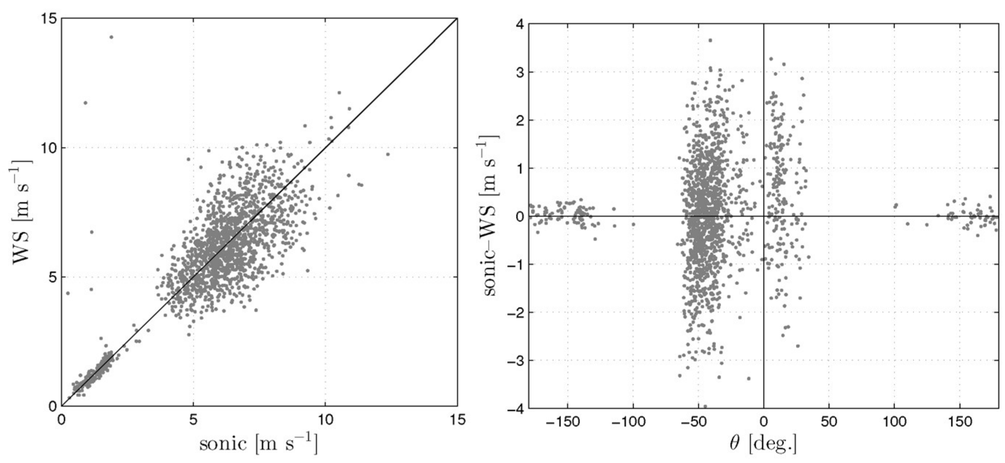


Figure 2: (Left) sonic and WS wind speed intercomparison. (Right) wind speed difference as a function of the relative direction

## Shelter results

The WS scanned on a vertical plane at 7 levels following the terrain. The speed up is shown in Fig. 3; although $\theta$ is not uniformly distributed, large differences in the shelter are noticed when varying $\theta$. Case I shows the deepest effect of the fence on the flow and for case IV the fence is only 'noticed' at $x/h \lessapprox 3$ ($h$ is the fence height). Case III shows a speed-up 'jump' region at $x/h \approx 2.5$ and $z/h \approx 2.5$. Such 'jump' is also found in CFD-RANS model simulations (not shown) and is due to increased vertical velocity shear in that region (a 'positive' effect of the fence on the wind). Case IV shows that $U(z)/U_o(z) \approx 1$ for $x/h \gtrapprox 4$, which indicates that there is a little effect of the topography on the flow at all scanning positions on the vertical plane compared to that at the mast position. Figure 3 also shows the direction and magnitude of the longitudinal velocity component measured by the WS. A region of reverse flow is visible below the shelter 'bubble' with the lowest speed ups. The magnitude of the reverse flow close to the fence, for case IV in particular, can be larger than the inflow value at the same vertical level. Preliminary comparisons with results from CFD-RANS and engineering obstacle models, such as that in WAsP (www.wasp.dk), reveal good agreement in the far wake ($x/h > 6$) and the need to include the distribution of $\theta$ in the model results.

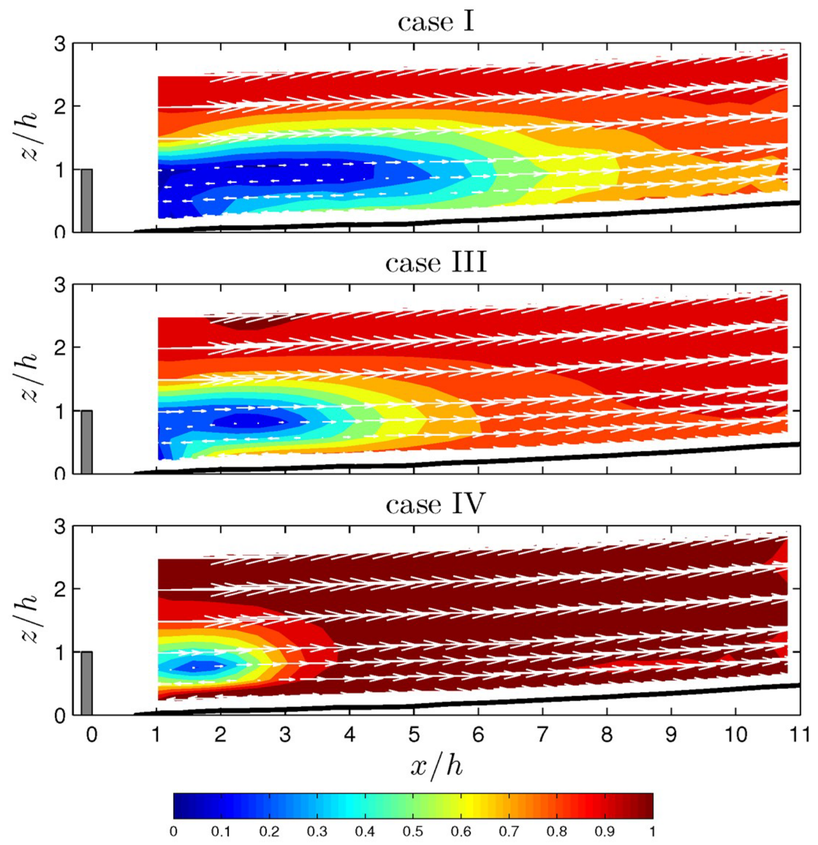


Figure 3: Speed up $U(z)/U_o(z)$ on the vertical plane behind the fence